The Deflagration - Detonation Transition in Gas-Fed Pulsed Plasma Accelerators

Article · July 2007

DOI: 10.2514/6.2007-5263

2 authors, including:

Nicolas Gascon
Stanford University
67 PUBLICATIONS **984** CITATIONS

SEE PROFILE

43rd AIAA/ASME/SAE/ASEE Joint Propulsion Conference & Exhibit
8 - 11 July 2007, Cincinnati, OH

AIAA 2007-5263

The Deflagration – Detonation Transition in Gas-Fed Pulsed Plasma Accelerators

Flavio Poehlmann[1], Nicolas Gascon[2], and Mark Cappelli[3]
Stanford University, Stanford, CA, 94305

A hydromagnetic Rankine-Hugoniot model for propellant acceleration in gas-fed pulsed plasma thrusters is presented and verified against available experimental data. Building on early work by Cheng et al [Nuclear Fusion 10, pp. 305-317, 1970], the snowplow mode is compared to a detonation process and it is shown here that a competing "second" mode, which was observed independently in gas-fed pulsed plasma thrusters by Ziemer et al [Ph.D. Dissertation, Princeton University, 2001], can be explained as a plasma deflagration process. Based on the presented model, a single equation is derived for these two modes, which gives the exhaust velocity of gas-fed pulsed plasma thrusters as a function of controllable parameters. It is found that the developed model is consistent with experimentally measured exhaust velocities for varying mass bit sizes.

Nomenclature

$\tilde{B}$	=	average azimuthal magnetic field
c^*	=	magnetosonic speed
c	=	speed of sound
e	=	internal energy
e^*	=	equivalent internal energy
f	=	magnetic field convection fraction
h	=	sensible enthalpy
h^*	=	equivalent sensible enthalpy
i	=	sum of sensible and chemical enthalpy
I	=	electric current
M^*	=	hydromagnetic Mach number
p	=	pressure
p^*	=	equivalent pressure
q	=	specific energy
T	=	temperature
u	=	gas velocity in wave frame
V	=	gas velocity in laboratory frame
α	=	detonation strength
γ	=	specific heat ratio
μ_0	=	permeability constant
v_A	=	Alfven velocity
ρ	=	density

I. Introduction

THE most commonly used model for the so-called Pulsed Plasma Thruster (PPT) is based on an electric circuit analysis and considers the plasma discharge as one part of the entire circuit[1,2]. While successful in predicting overall system performance, this model provides little physical insight to the mechanism by which the discharge

[1] Ph.D. Candidate, Mechanical Engineering, Building 520, AIAA Student Member.
[2] Research Associate, Mechanical Engineering, Building 520, AIAA Member.
[3] Professor, Mechanical Engineering, Building 520, AIAA Member.

accelerates the propellant. This paper presents a model for the acceleration mechanism in gas-fed PPTs that is derived from early work on coaxial plasma deflagration guns[3] and is based on an analogy of the processes involved in gas-fed pulsed plasma accelerators to chemical combustion waves. More specifically, the Rankine-Hugoniot theory for detonations and deflagrations can be extended to include magnetohydrodynamics in plasmas. A discussion of this theory can be found in the book by Sutton and Sherman[4]. In the hydromagnetic version of the Rankine-Hugoniot relation the three conservation laws are extended to also account for the magnetic pressure and magnetic energy, as well as for energy added to the flow from the capacitor bank. Carrying out the analysis with these modified equations leads to the replacement of the sound speed of the gas as a critical parameter that characterizes the flow by a speed that is a combination of both the sound and Alfvén speed.

Although first published in the 1960s, a study of current PPT literature suggests a lack of awareness of the early work of Cheng et al[3], which first gives references to the analogy between combustion wave and pulsed plasma wave dynamics. The following analysis is intended to build on the original model presented in Ref. 3, and to extend this theory to gas-fed PPTs. In addition, it seeks to verify the combustion wave analogy against experimental data published by Ziemer et al[5]. It is found that the magnetohydrodynamic equivalent of the Rankine-Hugoniot theory is in good agreement with the experimental observations and provides new physical insight to the acceleration mechanism. More importantly, it also explains a mode transition seen in these gas-fed pulsed plasma thrusters that occurs when the mass bit size is reduced below critical values.

This paper is structured the following way. Section II gives an overview of the Rankine-Hugoniot relation and how it is extended to the plasma case. In Section III, the theory is applied to gas-fed pulsed plasma thrusters and to explain the mode transitions observed when varying the mass-bit. Finally, in Section IV this theory is compared directly to experimental data published in Ref. 5. We conclude with a discussion of the physical insight gained from this novel way of treating this complex plasma flow.

II. Rankine-Hugoniot Theory

Figure 1a presents a schematic illustration of a one-dimensional (1-D) combustion wave that is traveling to the right at constant speed V_w. This wave is supported by combustion of a stationary unburned gas mixture to the right of this wave, resulting in the production of burned gas products on the left. The products move with a speed V_b dependent on the process considered. In the reference frame moving with this combustion wave, the unburned gas is moving into the wave at a speed of $-u_u$ (= $-V_w$) and the burned gas leaves the wave at a speed $-u_b$. We shall assume adiabatic flow, with heat release from the gas due to combustion within a narrow region about the wave front. The mixture densities ρ_u, ρ_b and pressures p_u, and p_b are uniform if evaluated far enough away from the combustion wave, and mass, momentum and energy balances can be applied across the wave. An appropriate equation of state (it is common in combustion theory to assume an ideal gas) gives a fourth equation, resulting in four equations for five unknowns u_u, u_b, p_b, ρ_b and the enthalpy i_b (the sum of chemical and sensible enthalpy).

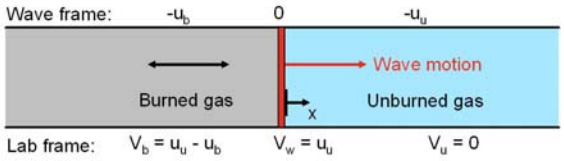

Figure 1a: One-dimensional illustration of a combustion wave inside a duct.

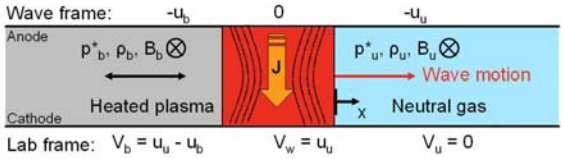

Figure 1b: One-dimensional plasma discharge inside a duct.

With slight modifications, this approach is also applicable to a non-reactive gas in a coaxial plasma accelerator. The gas is resistively heated by the discharge instead of through combustion. The pressures p_u and p_b also have a magnetic component in addition to the particle pressure and the energy equation has to be extended to include the magnetic field energy. These modifications can be made by introducing the equivalent pressure, p^*, and equivalent sensible enthalpy, h^*, given by Eqns. 1 and 2. Figure 1b illustrates the magnetic field and the one-dimensional discharge wave that is moving into the unprocessed neutral gas.

$$p^* = p + \frac{B^2}{2\mu_0} \tag{1}$$

$$h^* = e(p,T) + \frac{p}{\rho} + \frac{B^2}{2\mu_0\rho} = e^* + \frac{p^*}{\rho} \tag{2}$$

The mass, momentum and energy equations are then given by Eqns. 3, 4 and 5. In combustion, q is the chemical energy released during the reaction and is positive for an exothermic reaction. In the hydromagnetic case, q is the specific energy transferred from the capacitor bank to the plasma to resistively heat the gas and fill the electrode gap with magnetic field. Although no combustion takes place, the processed plasma will be referred to as the "burned" plasma so that the same subscripts can be used for the chemical and hydromagnetic cases. Since Eqns. 3 through 5 are fundamentally the same form as their combustion counterparts, all of the mathematical results from combustion theory carry over to this hydromagnetic analog of the Rankine-Hugoniot relation. For a rigorous derivation of the chemical Rankine-Hugoniot relation, the reader is referred to any combustion textbook, such as Ref. 6. References 3 and 4 can be consulted for more details on the hydromagnetic case.

Mass: $$\rho_u u_u = \rho_b u_b \tag{3}$$

Momentum: $$p_u^* + \rho_u u_u^2 = p_b^* + \rho_b u_b^2 \tag{4}$$

Energy: $$h_u^* + \frac{1}{2}u_u^2 + q = h_b^* + \frac{1}{2}u_b^2 \tag{5}$$

The mass and momentum equations can be combined to eliminate the burned gas velocity, u_b, resulting in the usual expression for the wave speed (in terms of the pressures and densities), commonly known as the Rayleigh line:

Rayleigh line: $$(\rho_u u_u)^2 = \left(\frac{p^*_b - p^*_u}{1/\rho_u - 1/\rho_b}\right) \tag{6}$$

The well known Hugoniot relation is obtained by eliminating the unburned gas velocity using the energy equation.

Hugoniot Relation: $$h_b^* - h_u^* = \frac{1}{2}\left(p^*_b - p^*_u\right)\left(\frac{1}{\rho_u} + \frac{1}{\rho_b}\right) + q \tag{7}$$

When represented on a graph of p^* versus $1/\rho$, the Hugoniot relation (see Fig. 2) gives the allowable combinations of burned gas pressure and density for specified unburned gas conditions, for particular values of h_b^* - h_u^* - q. Since the system is still underspecified, the pressure and density of the burned gas cannot be determined independently.

The solid curve in Fig. 2 gives the combinations of p_b^* and ρ_b that satisfy the three conservation laws. One can see that two sets of solutions exist, one for which the pressure and density increase across the wave and one for which they decrease. The former is commonly referred to as a *detonation*, while the latter is commonly called a *deflagration*. The part of the Hugoniot curve labeled V is an unphysical regime since an increase in pressure that is accompanied by a reduction in density would result in an imaginary wave speed (Eqn. 6).

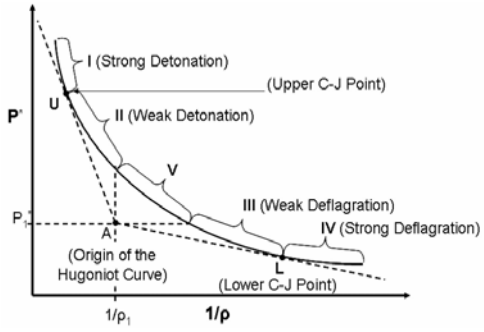

Figure 2: Hugoniot relation.

The difference between a detonation wave and a deflagration wave is often illustrated by way of the following thought experiment. One might imagine a pipe that is closed at one end, open at the other end, and filled with a combustible gas mixture. A detonation can be achieved by igniting the combustible mixture at the closed end. With no room to expand the pressure rises rapidly and causes a shock wave to travel through the unburned gas towards

the open end. The resulting compression-heating of the combustible mixture through the shock is sufficient to cause ignition. Since the shock travels faster than the ignition delay time, a detonation can be separated into two distinct parts, a thin shock followed by a thick heat release and expansion zone. Therefore, detonations are often modeled as a shock wave that is followed by a deflagration. A detonation has similarities to the snowplow mode observed in typical pulsed plasma thrusters. The current sheet originates at the closed end of the electrode gap and can be viewed as a hydromagnetic shock that ionizes and compresses unprocessed gas ahead of itself. The high magnetic pressure and temperature immediately behind the shock then accelerate the plasma. Similarities between a current sheet and a shock wave had already been pointed out by Burkhardt and Lovberg in 1962 based on magnetic field measurements[7].

In contrast to a detonation, a deflagration wave can be produced by igniting the gas mixture at the open end of the pipe. The wave travels upstream into the unburned gas to combust the mixture, while the combustion products are accelerated downstream. Unlike a detonation, the gas burned through the deflagration does not have to push against the unprocessed gas ahead of it. As a result, the burned gas pressure is slightly lower than the unburned gas pressure and the burned gas velocity is higher than that which can be achieved in a detonation. Compared to a detonation, a deflagration process deposits a higher fraction of the released combustion energy into the directed acceleration of the gas rather than into the heating of the gas. For a gas-fed pulsed plasma thruster, this translates into a higher exhaust velocity and higher thrust efficiency. It is shown later that a deflagration wave is a possible explanation for the mode transition observed in Ziemer's gas-fed PPT studies[5] and is the physical model proposed by Cheng[3] to explain the high exhaust velocities seen in his co-axial plasma accelerator.

A straight line originating from anywhere on the Hugoniot curve to point A in Fig.2, which defines the unburned gas state (p_u^*, $1/\rho_u$) has, as a slope, the right hand side of the Rayleigh line (Eqn. 6). As indicated in Eqn. 6, this slope is representative of the speed of the combustion wave. When the Rayleigh line is just tangent to the detonation branch of the Hugoniot curve, the allowable detonation wave speed reaches its minimum. This condition is called the Upper Chapman-Jouguet point, designated as "U" on the figure. Similarly, when the Rayleigh line is just tangent to the deflagration branch on the Hugoniot curve, the deflagration wave speed is at a maximum. This condition is called the Lower Chapman-Jouguet point, designated as "L" on the figure. For the combustion case, it can be shown that the burned gas velocity with respect to the wave is always the sonic speed at both Chapman-Jouguet points[6]. The same holds for the hydromagnetic case, with the modification that the sound speed is replaced by the magnetosonic speed c^*, defined in Eqn. 8. As shown in Eqn. 9, c^* can be expressed as a function of both the speed of sound, c, and the Alfvén speed, v_A.

$$c^* = \sqrt{\gamma \frac{p^*}{\rho}} \tag{8}$$

$$c^* = \sqrt{\frac{\gamma}{\rho}\left(p + \frac{B^2}{2\mu_0}\right)} = \sqrt{c^2 + \gamma v_A{}^2} \tag{9}$$

Considering the detonation and deflagration branches and the Chapman-Jouguet points on the Hugoniot curve, four regions are often defined, designated as I-IV in Fig. 2. Region I represents a strong detonation - a condition at which the unburned gas has a supersonic speed with respect to the wave and is decelerated to a subsonic speed through the shock. Strong detonations are allowable from both a first and second law perspective and can be achieved in practice. However, they require constant high energy addition and usually degenerate towards a Chapman-Jouguet detonation in the case of chemical combustion. Since a PPT uses an external power source which can provide more energy than is released in a combustion reaction, strong detonations are possible in these pulsed plasma thrusters. Weak detonations correspond to a solution for which the unburned gas is supersonic with respect to the wave and is decelerated to a lower supersonic speed. This violates the second law of thermodynamics and hence weak detonations do not occur.

Region IV corresponds to a strong deflagration - a condition in which the unburned gas has a subsonic speed with respect to the wave but is accelerated to supersonic speed by combustion. This is a second law violation since a gas cannot be accelerated to a supersonic speed in a constant area duct. Region III is a weak deflagration, which accelerates a subsonic gas to a higher subsonic speed. In combustion theory all deflagration waves are weak

deflagrations and a Chapman-Jouguet (C-J) deflagration at which the burned gas Mach number equals one can be approached in the limit. However, this requires constant high energy addition and therefore deflagrations in chemical combustion are usually very weak. This limitation does not necessarily apply to gas-fed pulsed plasma thrusters because of external energy supply. We expect therefore, to see these so-called C-J deflagrations.

III. Rankine-Hugoniot Theory applied to Gas-fed Plasma Thrusters

The hydromagnetic Rankine-Hugoniot theory from section II can be used to derive a single equation for the exhaust velocity of gas-fed PPTs. If the density and pressure in the neutral gas and burned plasma regions are known, the wave speed, u_u, can be calculated using the Rayleigh line expression (Eqn. 6). Then continuity can be used to find the burned gas velocity, which can then be transferred back to the stationary reference frame to give the exhaust velocity of the thruster. Therefore, the flow properties that need to be determined to calculate the exhaust velocity are the densities and pressures: ρ_u, ρ_b, p_u^* and p_b^*.

The neutral gas density, $\rho_{u,}$ is approximated from the mass bit and thruster dimensions. The burned gas density, ρ_b, can be found from the Hugoniot, which is simplified using the ideal gas approximation and assuming that the specific heat ratio γ is constant across the discharge region. Then the enthalpy terms in the Hugoniot can be expressed in terms of p^* and γ, as shown in Eqn. 10. The resulting expression is rearranged to solve for the density of the burned plasma (Eqn. 11).

$$\frac{\gamma}{\gamma-1}\left(\frac{p_b^*}{\rho_b}-\frac{p_u^*}{\rho_u}\right)-\frac{1}{2}\left(p_b^*-p_u^*\right)\left(\frac{1}{\rho_u}+\frac{1}{\rho_b}\right)=q \tag{10}$$

$$\rho_b=\frac{\frac{\gamma}{\gamma-1}p_b^*-\frac{1}{2}\left(p_b^*-p_u^*\right)}{q+\frac{\gamma}{\gamma-1}\frac{p_u^*}{\rho_u}+\frac{p_b^*}{2\rho_u}} \tag{11}$$

The determination of the remaining unknowns, p_b^* and p_u^*, varies depending on the thruster mode of operation and thus has to be treated separately. Since a detonation is essentially a deflagration behind a shock wave, the plasma deflagration is a fundamental concept underlying both modes of operation and is therefore described first.

A. Deflagration

Figure 3a shows a thruster operating in deflagration mode. The neutral gas enters the electrode gap from the left and travels to the right towards the discharge region. The discharge zone is moving upstream with respect to the neutral gas flow. Due to the strong magnetic field near the breech of the thruster, p_u^* can be approximated by the magnetic pressure alone because it is several orders of magnitude larger than the particle pressure.

The burned plasma pressure p_b^* is more difficult to determine. In the thick discharge region the flow is ionized and then resistively heated. As it expands, its collisionality decreases which causes the plasma magnetization to increase. As a result the magnetic Reynolds number R_M is likely to be close to or larger than one and a significant fraction of the magnetic field is convected downstream

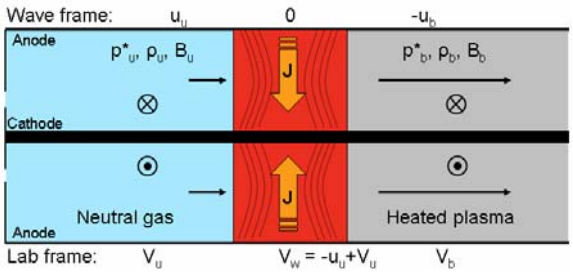

Figure 3a: One-dimensional plasma deflagration in a GF-PPT.

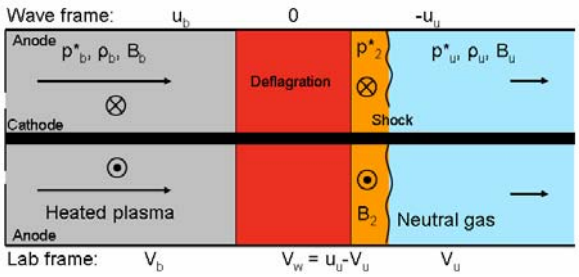

Figure 3b: One-dimensional plasma detonation in a GF-PPT.

with the plasma. Therefore, $p_b^* \approx f p_u^*$, where $0 \le f \le 1$. Unless the magnetic field convection fraction f is very small, p_b^* is again dominated by its magnetic component and the particle pressure can be neglected.

If f is known, the burned plasma velocity with respect to the wave can be found from the Rayleigh line and continuity equation. The exhaust velocity V_b is obtained by transferring u_b back into the stationary reference frame. Since deflagration waves move slowly, a good approximation is that $u_b >> V_u$ and therefore $V_b \approx u_b - u_u$. These results can be combined into a single expression for the exhaust velocity in terms of the known quantities ρ_u, q and γ, i.e.,

Exhaust Velocity (Deflagration):

$$V_b = \sqrt{(1-f)\frac{2q + \frac{\tilde{B}_u^{\,2}}{\mu_0 \rho_u}\left(\frac{\gamma(1-f)}{\gamma-1} + f + \frac{1}{2}\right)}{\frac{\gamma+1}{\gamma-1} f - 1}} \tag{12}$$

Additional parameters that are required are estimates of the average magnetic field, $\tilde{B}_u$, in the neutral gas region, and either the convection fraction f or an average magnetic field, $\tilde{B}_b$, in the burned plasma region. These can be easily measured, and future work may develop models to estimate these properties from first principles.

B. Detonation

The plasma detonation model can be used to calculate the exhaust velocity of a thruster that is operating in the snowplow mode. Analogous to combustion theory, the plasma detonation is treated as a hydromagnetic shock that travels downstream and is followed by a deflagration which expands the heated flow. Thus there are three regions of interest, which are shown in Fig. 3b. Region u contains the neutral gas downstream of the hydromagnetic shock, region 2 is immediately behind the shock but downstream of the deflagration and region b contains the burned plasma. Therefore, the analysis can be divided into two distinct steps. First, hydromagnetic shock jump conditions are used to determine the flow properties in region 2 as a function of the neutral gas properties in region u. Then the deflagration model is used to calculate the burned plasma properties as a function of the flow properties in region 2.

In the neutral gas region, the magnetic field is very weak and the pressure p_u^* is on the order of the particle pressure. As before, ρ_u is estimated from the mass bit size and the thruster dimensions. Then p_u^* can be found from the ideal gas law. The hydromagnetic shock compresses and ionizes the neutral gas and raises the pressure to p_2^*, which is dominated by its magnetic component. Consistent with the analogy to compressible flow, the shock jump condition for pressure rise across a shock is modified so that the Mach number is based on the magnetosonic speed c^* (Eqn. 13).

$$\frac{p_2{}^*}{p_u{}^*} = \frac{\tilde{B}_2^{\,2}}{2\mu_0 p_u{}^*} = \frac{\frac{2\gamma}{\gamma-1} M_u{}^{*2} - 1}{\frac{\gamma+1}{\gamma-1}} \tag{13}$$

Here, $\tilde{B}_2$ is the magnetic field immediately behind the shock and is averaged over time and radial position. If $\tilde{B}_2$ is known, Eqn. 13 can be solved for the hydromagnetic Mach number of the shock wave, M_u^*. $\tilde{B}_2$ can easily be found by experiment and future work may find ways to estimate it from first principles. With M_u^* known, the density jump across the shock can be calculated from Eqn. 14. As a result, the pressures and densities on both sides of the shock are known. Now the Rayleigh line relation and the continuity equation can be used to find u_u and u_2.

$$\frac{\rho_2}{\rho_u} = \frac{\frac{\gamma+1}{2} M_u{}^{*2}}{1 + \frac{\gamma-1}{2} M_u{}^{*2}} \tag{14}$$

With the pressure and density in region 2 known, the burned gas velocity with respect to the deflagration wave is calculated from the deflagration theory (discussed above). Since the hydromagnetic shock and deflagration waves must be moving in the same direction and must be at the same speed, the unburned gas speed with respect to the deflagration wave, u_2, is already determined.

The burned gas speed, u_b, depends on the strength of the deflagration process. For the case of a Chapman-Jouguet detonation, the deflagration behind the shock has to be of Chapman-Jouguet type. Otherwise u_b would not be magnetosonic. The shock decelerates the flow to sub-magnetosonic speed before the deflagration re-accelerates it to $M_b^* = 1$. Unlike the chemical combustion case, detonations in plasma accelerators are not limited to C-J detonations. The external power source can overdrive the system and make strong detonations possible[6]. In this case the burned plasma speed is sub-magnetosonic. This means that the flow behind the shock has been re-accelerated to a lesser extent. By definition then, a *strong* detonation consists of a shock that is followed by a *weak* deflagration.

As before, the strength of the deflagration is influenced by the magnetic field convection fraction f. However, the situation is complicated by the fact that the burned plasma is now inside the current loop of the thruster. Therefore, it is subject to the self-induced magnetic field from the cathode current and knowledge of f alone is not sufficient to estimate p_b^*. Instead, a new parameter, which is referred to as the detonation strength α, is introduced to express u_b as a fraction of the magnetosonic speed:

$$u_b = \alpha \sqrt{\gamma \frac{p_b^*}{\rho_b}} \tag{15}$$

For a Chapman-Jouguet detonation $\alpha = 1$ and for a strong detonation $\alpha < 1$. From continuity it follows that:

$$p_b^* = \frac{(\rho_2 u_2)^2}{\alpha^2 \gamma \rho_b} \tag{16}$$

which can be combined with the Rayleigh line to obtain ρ_b in terms of the flow properties in region 2, i.e.,

$$\rho_b = \frac{(\rho_2 u_2)^2 \left(\frac{\alpha^2 \gamma + 1}{\alpha^2 \gamma} \right)}{\rho_2 u_2^{\,2} + p_2^*} \tag{17}$$

If α is known, the burned plasma speed can be calculated by substituting Eqns. 16 and 17 into Eqn. 15. The exact value of α is difficult to determine analytically, but the range of allowable values can be found by determining its lower limit. Then $\alpha_{min} \le \alpha \le 1$, where α_{min} is always positive. From Fig. 2 it can be seen that the weakest allowable deflagration corresponds to a case where $p_b^* = p_2^*$. Using this approximation to eliminate p_b^* in Eqn. 15 and then substituting for ρ_b from Eqn. 17, the resulting expression can be solved for α_{min} :

$$\alpha_{\min} = u_2 \sqrt{\frac{\rho_2}{\gamma p_2^*}} \tag{18}$$

Since the shock is moving much faster than the neutral gas in front of it the burned plasma speed is transferred back to the stationary reference frame by making the approximation that $V_b \approx u_u - u_b$. Combining these results into a single expression yields the following equation for the upper and lower limits of the exhaust velocity, V_b.

Exhaust Velocity (Detonation):

$$V_b = \frac{p_2^* - p_u^* + \frac{\alpha^2 \gamma}{\alpha^2 \gamma + 1} \left(\frac{\rho_u}{\rho_2} p_u^* - p_2^* \right)}{\sqrt{\left(p_2^* - p_u^* \right) \rho_u \left(1 - \frac{\rho_u}{\rho_2} \right)}} \tag{19}$$

The required parameters ρ_u / ρ_2, p_2^* and α can be obtained from Eqns. 20 through 22:

$$\frac{\rho_u}{\rho_2} = \frac{4\gamma}{(\gamma+1)\left[\frac{p_2^*}{p_u^*}((\gamma+1)+(\gamma-1))\right]} + \frac{(\gamma+1)}{(\gamma-1)} \tag{20}$$

$$p_2^* = \frac{\tilde{B}_2^{\,2}}{2\mu_0} \tag{21}$$

$$\sqrt{\frac{p_2^* - p_u^*}{\left(\frac{1}{\rho_u/\rho_2} - 1\right)p_2^*\gamma}} \le \alpha \le 1 \tag{22}$$

IV. Verification against experimental Data

The plasma deflagration and detonation model developed in sections II and III is validated against experimental data from Ziemer et al[5]. In that study, the researchers measured the exhaust velocity of a gas-fed PPT as a function of mass bit size while keeping all other parameters constant. This experiment was conducted for several combinations of bank capacitance and total stored energy. Reference 5 reports a mode transition if the mass bit size is reduced below 0.5 μg that is characterized by a rapid increase in exhaust velocity and efficiency with decreasing mass bit size.

The hydromagnetic Rankine-Hugoniot theory from sections II and III can be applied to show that the *second* mode data is consistent with plasma deflagration theory, while the *regular* mode data lies within the upper and lower limits predicted by plasma detonation theory. This is shown in Fig. 4, which uses Ziemer's measurements[5] for a capacitance of 130 μF and a total energy of 4J. A discussion on how these curves were obtained is presented below.

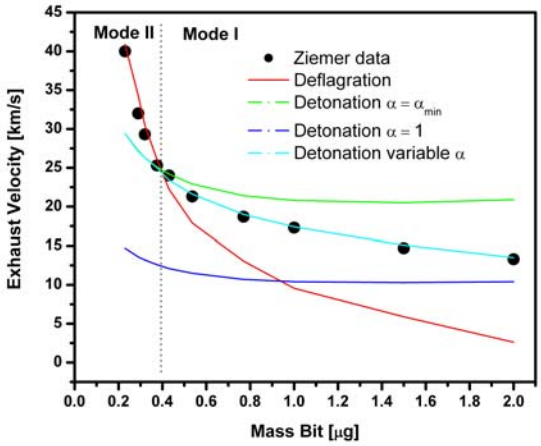

Figure 4: Deflagration and detonation theory versus experimental data for gas-fed PPT. Experimental data by Ziemer et al[5].

A. Mode II - Deflagration

The exhaust velocities for the deflagration branch that are shown in Fig. 4 were calculated using Eqn. 12. The required parameters ρ_u, q, γ, $\tilde{B}_u$ and f were determined using the following procedure.

The pulse timing of the gas-fed PPT was optimized to trigger breakdown as soon as the entire electrode gap was filled with gas[5]. Therefore, the density of the neutral gas, ρ_u, can be approximated by using the reported mass bit size divided by the volume between the electrodes, 290 cm^3. The specific heat addition, q, is derived from the energy, E, stored in the capacitor bank and is given by Eqn. 23. As is commonly the case in gas-fed PPTs, it is assumed that losses in the circuitry leave only 85% of E available to heat and magnetize the plasma.

$$q \approx .85\frac{E}{m_{bit}} \tag{23}$$

Since Argon was used as a propellant, the specific heat ratio of a monatomic ideal gas is used. Additional parameters that are required are the average magnetic field, $\tilde{B}_u$, in the neutral gas region and the magnetic field convection fraction, f. $\tilde{B}_u$ is estimated using the peak current measurements that Ziemer et al recorded along with the exhaust velocity data[5]. As can be seen in Fig. 5, the peak current during the deflagration mode is independent of mass bit size and is approximately 4.5kA for the data in series 2. Treating the current waveform of each pulse as

sinusoidal, the average current is taken to be one-half the peak current. With this, the average magnetic field strength is estimated using:

$$\tilde{B}_u = \frac{\mu I_{peak}}{4\pi R_t} \tag{24}$$

which treats the gas-fed PPT as a toroid with a radius of R_t = 2.5 cm. For the case of series 2, this yields a space and time averaged magnetic field of 20 mT.

The parameter that remains to be determined is the magnetic field convection fraction *f*. For the purposes of this study, *f* is determined by fitting the developed model to the experimental data. Since the conductivity of the plasma increases with number density, *f* has to increase with mass bit size. Good agreement is found if the convection fraction for a 0.23μg-mass bit is $f = 0.88$ and increases monotonically to $f = 0.92$ for a 0.38μg-mass bit. For mass bit sizes above 0.38μg the deflagration model no longer yields results that agree with the experimental data. This supports the hypothesis that a mode transition takes place at this point.

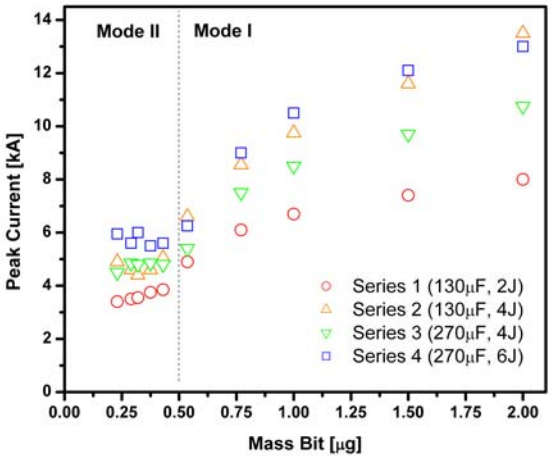

Figure 5: Peak current versus mass bit size. Data by Ziemer et al[5].

B. Mode I - Detonation

The upper and lower limits for the exhaust velocity of the detonation branch are calculated from Eqns. 19-22. The parameters γ, q and ρ_u are determined in the same way as for the deflagration branch. The unburned gas pressure, p_u is approximated using the ideal gas law based on ρ_u and room temperature.

The last parameter that needs to be determined is the average magnetic field strength behind the shock, $\tilde{B}_2$. Since $\tilde{B}_2$ is the magnetic field in a narrow region immediately behind the shock and is expected to be larger than $\tilde{B}_b$, it is not possible to estimate $\tilde{B}_2$ from Eqn. 24. Nevertheless, $\tilde{B}_2$ should still be proportional to the current so that the following general expression is used:

$$\tilde{B}_2 = C \times I_{peak} \tag{25}$$

Here, *C* is a constant (discussed below). As was done for the deflagration case, the peak current is taken from Ziemer's data shown in Fig. 5. For the detonation branch the maximum current is no longer independent of mass bit size but varies with it almost linearly.

The constant *C* in Eqn. 25 is determined by fitting the model to the first data point of the detonation branch. Although the exact mechanism governing deflagration-to-detonation transition (DDT) is not fully understood, it is commonly observed in combustion applications that the DDT results in a strong detonation that then degenerates towards a Chapman-Jouguet detonation[8,9]. It is assumed that the same holds true for the case of the hydromagnetic analog and hence that $\alpha = \alpha_{min}$ for the 0.43μg-mass bit. This yields $\tilde{B}_2 = 54mT$ and thus a value of $C = 0.008T/kA$. The magnetic field strength of 48mT appears reasonable as it is the same order of magnitude as the average magnetic field strength in the deflagration branch and consistent with commonly observed data for gas-fed PPTs[10].

As the mass bit size is increased, the specific energy, *q*, decreases and it is expected that the detonation approaches a Chapman-Jouguet detonation for which $\alpha = 1$. At the moment the model cannot yet account for this effect. Instead, an upper and lower limit for the exhaust velocity is given corresponding to the cases $\alpha = \alpha_{min}$ and $\alpha = 1$. Figure 4 shows that the experimentally measured exhaust velocities are within these limits and follow the expected trend from a strong detonation towards a Chapman-Jouguet detonation. Alternatively, the calculated results for the detonation branch can be matched to the experimental data by increasing α monotonically towards 1.

V. Discussion

The plasma deflagration and detonation models developed in sections II and III are consistent with the experimental data presented in section IV. For the deflagration branch the magnetic field convection fraction f was found from fitting the model to experimental data. This is also the case for the detonation branch, where the average magnetic field behind the hydromagnetic shock, $\tilde{B}_2$, was determined in a similar way. This means that a free parameter is purposely selected to force the model onto given data points and thus it cannot be ruled out (although it is unlikely) that the good agreement with experimental data is merely coincidental. Therefore, future work should verify the values used for f and $\tilde{B}_2$, either experimentally or by developing models to determine them from first principles. Nevertheless, both f and $\tilde{B}_2$ needed to fit the data are found to be reasonable and are consistent with commonly reported gas-fed PPT data[10]. They also follow the expected trends, such as the increase in f with mass bit size.

Despite its dependence on experimental data, the hydromagnetic Rankine-Hugoniot approach provides valuable physical insights into the plasma acceleration process. Current PPT theory leaves gaps in the physical understanding of the interaction mechanism between the discharge current and the accelerated gas. The plasma detonation and deflagration model complements PPT theory well since it is derived from a clear physical description of the process by which the discharge accelerates the propellant.

In addition, the hydromagnetic Rankine-Hugoniot theory offers an explanation to Ziemer's observation that a second mode exists in gas-fed PPTs for mass bit sizes below a critical value. This second mode is characterized by a strong inverse dependence of specific impulse and thrust efficiency on mass bit size. In chemical combustion, a deflagration consists of a reaction zone that moves upstream and processes the incoming reactants rather than pushing them ahead of itself as would be the case for a detonation. Similarly, a plasma deflagration is characterized by an ionization zone that moves upstream with respect to the propellant. This is especially intuitive if one considers that ionization by electron collision is essentially equivalent to a chemical reaction, with the difference that the colliding reactants are a free electron and a neutral instead of fuel and oxygen molecules.

As was explained in section II, a detonation is initiated by igniting the combustible gas mixture inside a tube at its closed end while a deflagration is ignited at its open end. The collision frequency of the gas particles thus determines the mode of combustion. This is consistent with Ziemer's observation that a reduction in mass bit size triggers the mode transition. It is hypothesized that the mode transition is linked to either the Knudsen number or the Hall parameter becoming greater than one as the mass bit is reduced. In both cases, collisions become negligible and the situation is essentially identical to the one at the open end of a tube. In order to maintain the deflagration mode, the voltage across the electrodes has to remain high enough so that continuous breakdown can occur upstream of the moving discharge. This requires high discharge impedance, which may be provided by the fast time change of total inductance due to the fast acceleration of the plasma.

VI. Conclusion

A model for gas-fed pulsed plasma thrusters is presented that is based on a hydromagnetic analog to the Rankine-Hugoniot theory from chemical combustion theory. Current gas-fed PPT theory is mainly based on an electric circuit analogy and empirical scaling laws. The relations developed in this paper supplement existing theory by providing a model that is derived from a physical description of the interaction between the discharge and the accelerated gas. The model is validated against experimental data from Ziemer et al[5]. Certain parameters that are required for the model still have to be obtained by fitting the model to experimental data. Future work will verify the fitted parameters. The hydromagnetic Rankine-Hugoniot theory supports Ziemer's observation that a high efficiency, high specific impulse mode is accessible in a gas-fed PPT and suggests that this transition is governed by a reduction of collisionality in the discharge region.

Acknowledgments

The authors would like to extend their appreciation to Prof. D.Y. Cheng, for stimulating discussions, the donation of equipment, and for introducing us to the plasma deflagration propulsion concept. We would also like to thank Prof. E. Choueiri and Dr. J. Ziemer for bringing the mode transition observed in their experiments to our attention and for the stimulating discussions. We also would like to acknowledge Dr. J.-L. Cambier (AFRL) for providing needed

equipment, Dr. M. A. Birkan (Air Force) for funding this work through an STTR subcontract, and Dr. J. Szabo at Busek Inc. for collaborating on the development of the CHENG thruster.

References

[1]Jahn, R.G., "Physics of Electric Propulsion", Ch. 9, McGraw-Hill Series in Missile and Space Technology, New York: McGraw-Hill Book Company, 1968

[2] Ziemer, J.K., Choueiri, E.Y., "Scaling Laws for Electromagnetic Pulsed Plasma Thrusters", Plasma Sources Science and Technology, 10(3): 395-405, Aug. 2001

[3]Cheng, D.Y., "Plasma Deflagration and the Properties of a Coaxial Plasma Deflagration Gun", Nuclear Fusion 10, pp. 305-317, 1970

[4]Sutton, G.W., Sherman, A., "Engineering Magnetohydrodynamics", Ch.9, McGraw-Hill, 1965

[5]Ziemer, J.K., "Performance Scaling of Gas-Fed Pulsed Plasma Thrusters", PhD Dissertation, Princeton University, 2001

[6]Kuo, K.K., "Principles of Combustion", pp. 231-284, John Wiley and Sons, 1986

[7]Burkhardt, L.C., Lovberg, R.H., "Current Sheet in a Coaxial Plasma Gun", The Physics of Fluids V.5, #3, pp. 341-347, 1962.

[8]Smirnov, N.N., Nikitin, V.F., "Fundamentals of Deflagration to Detonation Transition in Gases", Proceedings of 19th International Colloquium on the Dynamics of Explosions and Reactive Systems (ICDER), 2003

[9]Smirnov, N.N., Nikitin, V.F., "Effect of Channel Geometry and Mixture Temperature on Detonation-to-Deflagration Transition in Gases", Combustion, Explosion, and Shock Waves, V.40 #2, pp. 186-199, 2004

[10]Makusic, T.E., Choueiri, E.Y., "Photographic, Magnetic, and Interferometric Measurements of Current Sheet Canting in a Pulsed Electromagnetic Accelerator", AIAA 2001-3896